PHYSICAL REVIEW B **83**, 155431 (2011)

Fluctuation theorem and microreversibility in a quantum coherent conductor

Shuji Nakamura,[1] Yoshiaki Yamauchi,[1] Masayuki Hashisaka,[1] Kensaku Chida,[1] Kensuke Kobayashi,[1,*] Teruo Ono,[1] Renaud Leturcq,[2] Klaus Ensslin,[3] Keiji Saito,[4] Yasuhiro Utsumi,[5] and Arthur C. Gossard[6]

[1]*Institute for Chemical Research, Kyoto University, Uji, Kyoto 611-0011, Japan*

[2]*Institute of Electronics, Microelectronics and Nanotechnology, CNRS - UMR 8520, Department ISEN, Avenue Poincaré, F-59652 Villeneuve d'Ascq, France*

[3]*Solid State Physics Laboratory, ETH Zürich, CH-8093 Zürich, Switzerland*

[4]*Graduate School of Science, University of Tokyo, Tokyo 113-0033, Japan*

[5]*Department of Physics Engineering, Mie University, Mie 514-8507, Japan*

[6]*Materials Department, University of California, Santa Barbara, California 93106, USA*

(Received 30 January 2011; revised manuscript received 23 March 2011; published 18 April 2011)

Mesoscopic systems provide us a unique experimental stage to address nonequilibrium quantum statistical physics. By using a simple tunneling model, we describe the electron exchange process via a quantum coherent conductor between two reservoirs, which yields the fluctuation theorem (FT) in mesoscopic transport. We experimentally show that such a treatment is semiquantitatively validated in the current and noise measurement in an Aharonov-Bohm ring. The experimental proof of the microreversibility assumed in the derivation of FT is presented.

DOI: 10.1103/PhysRevB.83.155431 PACS number(s): 05.40.−a, 72.70.+m, 73.23.−b, 85.35.Ds

I. INTRODUCTION

Since the 1980s mesoscopic conductors have been serving as an ideal stage to investigate the quantum scattering problem both theoretically and experimentally, because the quantum transport through a single site can be precisely probed in electronic measurement.[1] The Landauer-Büttiker formalism embodies this advantage of mesoscopic physics, as was successfully applied to the Aharonov-Bohm ring, the quantum point contact, and the quantum dot, through which the mesoscopic physics has been established [see Fig. 1(a)]. Not only the current averaged over for a certain time ($\langle I \rangle$), but also the current fluctuation $\langle (\delta I)^2 \rangle$ due to the partition process is treated in the same framework.[2–4] Actually, the quantum shot noise measurement was successfully demonstrated, for example, to provide the direct proof of the fractional charge[5,6] and the Cooper pair[7] by looking at how carriers are scattered at a mesoscopic conductor.

These days the mesoscopic transport is invoking much interest from another point of view. As the electron transport can be viewed as the electron exchange process between the reservoirs via the conductor as shown in Fig. 1(b), it serves as a well-defined test stage for nonequilibrium quantum statistical physics.[8] The unique advantage of this approach lies in that the degree of nonequilibrium can be finely tuned by the bias voltage applied to the conductor. In addition, many events, namely numerous electron exchange processes, can be monitored, which enables us to perform precise measurement.

To quantitatively address the above topic, the fluctuation theorem (FT)[9] is believed to play a central role.[8,10–18] Based on microscopic reversibility ("microreversibility" or detailed balance), this relation exactly links the probabilities of the production and consumption of the entropy in a given system that is coupled to the reservoir. FT corresponds to a microscopic expansion of the macroscopic second law of thermodynamics and is proven to yield the linear-response theory[19] and the Onsager-Casimir relations.[13] FT was experimentally proved to be valid in classical systems such as a colloidal particle in fluid[20] and a resistor.[21] Although it was extended to the quantum regime,[22] an experimental check in this regime was still lacking. More recently, FT was theoretically addressed in the mesoscopic transport[10–12,16–18] even in the presence of the magnetic field[13–15] and was indeed shown to be relevant in the analysis[16] of the electron counting experiments.[23,24] While the incoherent tunneling events across the quantum dot(s) were investigated in the above experiments, the validity of FT in the quantum coherent regime was left to be addressed.

Recently, we experimentally showed the presence of nontrivial relations between the nonlinear response and the nonequilibrium fluctuation in the coherent transport of an Aharonov-Bohm (AB) ring.[25] When the current I and the current fluctuation (current noise power spectral density) S are expanded in the Taylor series as a polynomial of the bias voltage V,

$$I(V,B) = G_1(B)V + \frac{1}{2!}G_2(B)V^2 + \frac{1}{3!}G_3(B)V^3 + \cdots \quad (1)$$

and

$$S(V,B) = S_0(B) + S_1(B)V + \frac{1}{2!}S_2(B)V^2 + \cdots, \quad (2)$$

we showed that there are proportional relations of $S_1^S \propto G_2^S$ and $S_1^A \propto G_2^A$. Here, the coefficients that are symmetrized (S) or antisymmetrized (A) with respect to the magnetic field reversal are defined as

$$G_2^{S,A}(B) \equiv G_2(B) \pm G_2(-B) \quad (3)$$

and

$$S_1^{S,A}(B) \equiv S_1(B) \pm S_1(-B) \quad (4)$$

(take $+$ and $-$ for S and A, respectively). This result is beyond the consequence of the fluctuation-dissipation theorem $S_0(B) = 4k_BTG_1(B)$. Our observation semiquantitatively agrees with the theoretical prediction on the basis of FT[13] and provides an evidence of FT in the nonequilibrium quantum regime.

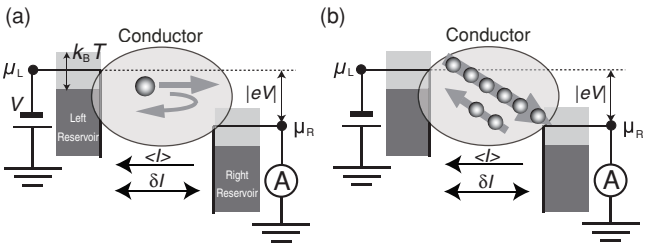

FIG. 1. (a) Schematic picture of the mesoscopic conductor coupled to the two reservoirs in the nonequilibrium regime. μ_L and μ_R are the chemical potentials of the left and the right reservoirs, respectively. Mesoscopic transport based on the Landauer-Büttiker picture is schematically shown. When a conductor is biased, electrons injected from one of the reservoirs are either transmitted or reflected at the conductor, which yields finite current fluctuation $[\langle(\delta I)^2\rangle \neq 0]$. (b) The transport can be also viewed as the electron exchange process between the two reservoirs.

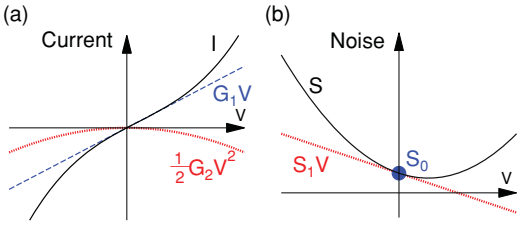

FIG. 2. (Color online) (a) Current-voltage characteristic as a function of the bias voltage V. While Ohm's law holds around $V = 0$, the current I is not linear at large V and the I-V characteristics can be decomposed into a polynomial of V with coefficients $G_1, G_2, G_3, \ldots$ as in Eq. (1). In this study we address G_2. This schematic graph shows the total current I, the G_1V contribution, and the $1/2!G_2V^2$ contribution, in the solid, dashed, and dotted curves, respectively. The case with a negative G_2 is shown. (b) Similarly, the current noise spectral density S (shown in the solid curve) can be expressed in a polynomial form of V as in Eq. (2). The Johnson-Nyquist relation tells that $S(V = 0) = S_0 = 4k_BTG_1$. This schematic graph shows the case with a negative S_1 in the dashed curve. Here we address the coefficient of the term linear in V (S_1) and the relation between S_1 and G_2.

In this paper we expand the above work to further support our previous report. In Sec. II, based on a simple tunneling model, we derive FT in an applicable form to simple mesoscopic conductors. In Sec. III we discuss the breakdown of the Onsager-Casimir reciprocity in the nonequilibrium regime in the presence of the magnetic field. Then, as a fundamental aspect of FT in mesoscopic transport, we show that the validity of the microreversibility can be directly addressed in a quantum regime.

II. FLUCTUATION THEOREM IN A MESOSCOPIC SYSTEM

A. Zero-magnetic field case

We explain FT by using the simplest setup and deduce the aforementioned nonequilibrium fluctuation relations. We consider a mesoscopic conductor, say a quantum point contact, where the two quantum wires are coupled by tunneling. While more systematic and general derivation for these relations is performed by using a cumulant generating function,[12–18] the present simplest model is sufficiently instructive to treat here. We assume that no energy relaxation takes place inside the conductor, which is fulfilled in many mesoscopic devices smaller than the energy relaxation length such as a quantum dot (QD), chaotic cavity, ring, and so on. First we treat the zero-magnetic field case to show $S_1 = 2k_BTG_2$ in Eqs. (1) and (2). The relations between the coefficients in the current and the current noise are schematically shown in Fig. 2.

The present system is described by the following Hamiltonian:

$$H = H_L + H_R + H_{LR}, \tag{5}$$

where H_L and H_R are the Hamiltonian of the left and right quantum wires and H_{LR} is the tunneling part between them. The initial density matrix is decoupled into the equilibrium states of each wire, where the left and right wires are assumed to have equal temperature $1/\beta = k_BT$ and have chemical potentials μ_L and μ_R, respectively. Then the whole density matrix is described by

$$\hat{\rho}_{\text{initial}} = \sum_{n_L,n_R} \rho_{n_L,n_R} |n_L,n_R\rangle\langle n_L,n_R|, \tag{6}$$

$$\rho_{n_L,n_R} = \frac{e^{-\beta[E_{n_L}-\mu_L n_L]}}{Z_L} \frac{e^{-\beta[E_{n_R}-\mu_R n_R]}}{Z_R}, \tag{7}$$

where Z_L and Z_R are the normalization factors and $|n_L,n_R\rangle$ defines the state that n_L and n_R electrons are present inside the left and right wires with the eigenenergies E_{n_L} and E_{n_R} of H_L and H_R, respectively.

The probability of finding the state $|n'_L,n'_R\rangle$ after a certain time τ starting from the initial state $|n_L,n_R\rangle$ is expressed as

$$P_{(n_L,n_R)\to(n'_L,n'_R)} = |\langle n'_L,n'_R|e^{\frac{-i\tau}{\hbar}H}|n_L,n_R\rangle|^2 \rho_{n_L,n_R}.$$

The microreversibility or the time reversal symmetry is given by

$$|\langle n'_L,n'_R|e^{\frac{-i\tau}{\hbar}H}|n_L,n_R\rangle|^2 = |\langle n_L,n_R|e^{\frac{-i\tau}{\hbar}H}|n'_L,n'_R\rangle|^2.$$

Here for simplicity we assume that $|n_L,n_R\rangle$ and $|n'_L,n'_R\rangle$ has the time reversal symmetry as the electron numbers are the good quantum number, while in the general treatment[13] this assumption is not necessary.

As the electron number conservation $n_L - n'_L = -(n_R - n'_R)$ and the energy conservation are satisfied at very large τ, $E_{n'_L} - E_{n_L} \approx -(E_{n'_R} - E_{n_R})$. Using the microreversibility and the conservation laws, we find the relation

$$P_{(n_L,n_R)\to(n'_L,n'_R)} = P_{(n'_L,n'_R)\to(n_L,n_R)} e^{A(n_L-n'_L)},$$

where A is an affinity $A = \beta(\mu_L - \mu_R)$. The probability that the number of the transmitted electron is Q, is defined as $P(Q) = \sum_{n_L,n_R,n'_L,n'_R} P_{(n_L,n_R)\to(n'_L,n'_R)} \delta[Q - (n_L - n'_L)]$. Therefore, FT is obtained as the direct consequence of the microreversibility

$$P(Q) = P(-Q)e^{AQ}. \tag{8}$$

This microreversibility ensures the following sum rule, which is called "global detailed balance" in Ref. 14,

$$\langle e^{AQ}\rangle = 1, \tag{9}$$

since $1 = \sum_Q P(Q) = \sum_Q P(-Q)e^{AQ} = \langle e^{AQ}\rangle$. Here $\langle\cdots\rangle$ denotes the expectation $\langle\cdots\rangle \equiv \sum_Q \cdots P(Q)$.

Now let us discuss the higher order correlations between the current and its noise power, which are the central topic in the present paper. With FT (8), we find the following identity:

$$\langle Q\rangle = \sum_Q Q P(Q) = -\sum_Q Q P(Q)e^{-AQ}$$
$$= -\langle Q\rangle + A\langle Q^2\rangle - \frac{A^2}{2!}\langle Q^3\rangle + \cdots. \quad (10)$$

Furthermore, we note that $\langle Q^n\rangle$ can be expanded in the Taylor series of A with the coefficients $\langle Q^n\rangle_m$ (n,m integer)

$$\langle Q^n\rangle = \langle Q^n\rangle_0 + A\langle Q^n\rangle_1 + \frac{A^2}{2!}\langle Q^n\rangle_2 + \cdots. \quad (11)$$

Comparing order by order with respect to A, we find infinite number of relationships among these coefficients, some of which are given as

$$\langle Q^2\rangle_0 = 2\langle Q\rangle_1, \quad (12)$$
$$\langle Q^2\rangle_1 = \langle Q\rangle_2. \quad (13)$$

Averaged current I and current noise power S are defined as $I = \langle Q\rangle/\tau$ and $S = 2(\langle Q^2\rangle - \langle Q\rangle^2)/\tau$.[26] The first relation (12) is equivalent to the fluctuation dissipation relations[19]

$$S_0 = 4k_B T G_1, \quad (14)$$

and the second relation (13) is to

$$S_1 = 2k_B T G_2. \quad (15)$$

This relation is beyond the fluctuation-dissipation relation and directly links the nonlinearity and the nonequilibrium of the system.

B. Finite magnetic field case

At $B \neq 0$ the microreversibility requires that the probability $P(Q,B)$ should satisfy[13]

$$P(Q,B) = P(-Q,-B)\exp(AQ). \quad (16)$$

$P(Q,B)$ is now decomposed to the symmetric and antisymmetric parts regarding the magnetic field reversal $P_\pm(Q) \equiv P(Q,B) \pm P(Q,-B)$, which fulfill

$$P_\pm(Q) = \pm P_\pm(-Q)e^{AQ}. \quad (17)$$

Although the symmetric part $P_+(Q)$ produces the same fluctuation relations as $P(Q)$ does, the antisymmetric probability gives rise to a nontrivial result. By considering the antisymmetrized number of charges exchanged between the reservoirs,

$$\langle Q_-\rangle \equiv \sum_Q Q P_-(Q) = \sum_Q Q P_-(Q)e^{-AQ} \quad (18)$$

and defining $\langle Q_-^n\rangle_m$ with nonnegative integers n and m as the coefficients in the Taylor expansion of the above $\langle Q_-\rangle$ with regard to A, we obtain

$$\langle Q_-^3\rangle_0 = 2\langle Q_-^2\rangle_1. \quad (19)$$

By noting the following relation, which is the consequence of the normalization condition $\sum_Q P(Q) = 1$:

$$0 = \sum_Q P_-(Q) = -\sum_Q P_-(Q)e^{-AQ}, \quad (20)$$

we obtain

$$3\langle Q_-\rangle_2 - 3\langle Q_-^2\rangle_1 + \langle Q_-^3\rangle_0 = 0. \quad (21)$$

The current that is antisymmetrized with regard to the B reversal is defined as $I(V,B) - I(V,-B) = \langle Q_-\rangle/\tau$ and the current noise power is also defined in the same way, Eqs. (19) and (21) yields

$$S_1^A = C_0^A/2k_B T \quad (22)$$

and

$$S_1^A - 2k_B T G_2^A = C_0^A/3k_B T, \quad (23)$$

respectively. Here C_0^A, which originates from the term $\langle Q_-^3\rangle_0$, is the antisymmetric part of the third cumulant at equilibrium. These two yield the antisymmetric relation expressed by

$$S_1^A = 6k_B T G_2^A. \quad (24)$$

The above deduction totally relies on the microreversibility as is the case in a systematic derivation.[13] Recently, however, an interesting possibility of the broken microreversibility in mesoscopic conductors is pointed out.[14,15] It was discussed that, because of the global detailed balance expressed by Eq. (9), the sum rule Eq. (20) and hence Eq. (21) hold true without microreversibility, even if we do not resort to the relation $P_-(Q) = -P_-(-Q)\exp(AQ)$ [Eq. (16)]. In this case, Eq. (19) and the resultant Eq. (22) are no more valid and only Eq. (23) is expected. To address this issue experimentally is the main motivation of the present paper.

The conventional current and shot noise formulas in the Landauer-Büttiker framework can be also expressed in the polynomial form of V {see Eqs. (39) and (61) in Ref. 4}. By taking the energy-dependent transmission into account, a relation similar to Eq. (15) holds true. However, this approach, which is based on the transmission defined in the equilibrium, fails to explain the nonlinear conductance that is not symmetric with respect to the magnetic field reversal. Indeed, it is established theoretically and experimentally[27–31] that due to electron-electron interactions induced in biased mesoscopic conductors, the Onsager-Casimir reciprocal relations are broken, leading to finite G_2^A. We will show the experimental data regarding this below.

III. MAGNETIC FIELD ASYMMETRY AND MICROREVERSIBILITY

A. Experiment

We used an Aharonov-Bohm (AB) ring as a typical coherent conductor. Figure 3(a) shows an atomic force microscope (AFM) image of the AB ring fabricated by local oxidation using an AFM[33] on a GaAs/AlGaAs heterostructure two-dimensional electron gas (2DEG) (the electron density 3.7×10^{11} cm^{-2}, the mobility 2.7×10^5 cm^2/V s and the electron mean free path 2.7 μm). The two-terminal current and noise measurement setup in a dilution refrigerator is also shown in

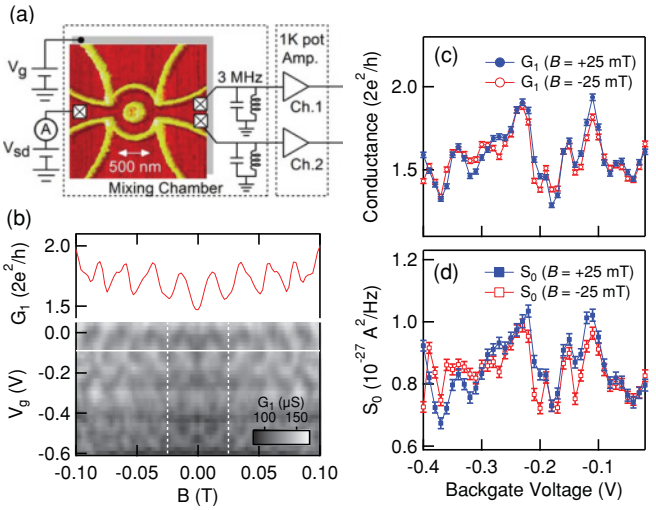

FIG. 3. (Color online) (a) Atomic force microscope (AFM) image of the AB ring fabricated by local oxidation using an AFM[33] on a GaAs/AlGaAs 2DEG with the experimental setup for the two-terminal current and noise measurements. (b) Image plot of the conductance of the ring as a function of V_g and B (in the lower panel). The upper panel shows the magnetoconductance at $V_g = -0.09$ V as indicated by a white line in the lower panel. (c) Conductance as a function of V_g at $B = \pm 25$ mT [indicated by dashed lines in the lower panel of (b)]. (d) Equilibrium noise (S_0) as a function of V_g at $B = \pm 25$ mT.

Fig. 3(a). The in-plane gates defined by the oxide lines are grounded in the present measurement. The 2DEG has a back gate to tune the electron density and the conductance of the AB ring can be modulated by the back gate voltage V_g and the magnetic field B by the AB effect. Figure 3(b) shows the image plot of the conductance as a function of V_g and B. The upper panel of Fig. 3(b) presents the conductance at $V_g = -0.09$ V displaying clear AB oscillations with an oscillation period being 25 mT in agreement with the ring radius of 230 nm.[31,32] The conductance of the ring ranges between 1.3 and 1.7 in units of $2e^2/h \sim (12.9\ \mathrm{k}\Omega)^{-1}$ with typical visibility of ~0.13. The presence of electron interferences guarantees the coherent electron transport in the device.

In addition to the dc measurement, we performed the noise measurement as follows [also see Fig. 3(a)]. The voltage fluctuation across the sample on the resonant circuit, whose resonant frequency is about 3.0 MHz with the bandwidth of ~140 kHz, is extracted as an output signal of the cryogenic amplifier.[5,25,34–36] The time-domain signal is then captured by the two-channel digitizer, and is converted to spectral density data via FFT. To increase the resolution of the noise spectrum, we performed the cross-correlation technique by using two sets of resonant circuit and amplifier. The sample was placed in a dilution refrigerator whose base temperature is 45 mK and the electron temperature in the equilibrium was 125 mK as deduced from the thermal noise. By numerically fitting the obtained resonant peak, the current noise power spectral density S is obtained as performed in Ref. 34.

In the analysis of the current I and the current noise S as polynomials of V, the bias window was set to $|eV| \leqslant 50\ \mu$eV, which corresponds to $4.6k_BT$ at $T = 125$ mK. In this bias range, the Joule heating is expected to be negligible as seen in previous shot noise measurements for mesoscopic devices.[35,36] The coefficients in Eqs. (1) and (2) are deduced from the numerical fitting to the obtained current and current noise. The polynomial fitting for I and S was performed by taking up to the fifth order of V for I and up to the fourth order of V for S into account, respectively. The analysis up to third or seventh order of V for I and second order of V for S yields results consistent with those presented below. We note that the measurement was carefully performed at several different V_g and B, and all the results are in a quantitative agreement with each other within the experimental accuracy of the present work.

B. Results and Discussions

Figure 3(c) shows the zero-bias conductance G_1 obtained at $B = 25$ mT and $B = -25$ mT at 125 mK as a function of the back gate voltage V_g. Since V_g modulates the electron density in the ring, hence the interference pattern, the conductance fluctuates as V_g varies. As the Onsager-Casmir reciprocity tells, G_1 behaves similarly at $B = 25$ and -25 mT as V_g changes. The correlation factor (CF) between the two, which is the covariance of the two divided by the product of their standard deviations, is 0.91. Similarly, as shown in Fig. 3(d) the gate-dependent thermal noises (S_0) at $B = 25$ mT and -25 mT lap over each other with CF = 0.68. Also we note that the proportionality between G_1 and S_0 indicates that $S_0 = 4k_BTG_1$ holds with an electron temperature of $T = 125$ mK. The coefficients of the first term in Eqs. (1) and (2) satisfy the Onsager-Casimir reciprocity as a fundamental property in the equilibrium.

Next we discuss the coefficients in the second term of Eqs. (1) and (2). Figures 4(a) and 4(b) show G_2 and S_1 at $B = 25$ and -25 mT, respectively. It is remarkable that unlike the equilibrium property (G_1 and S_0), G_2 and S_1 are not symmetric with respect to the magnetic field reversal. Indeed CFs between the traces for the negative and positive fields are as low as 0.20 and 0.38 for G_2 and S_1, respectively. Regarding G_2, the presence of this asymmetry was reported recently as the signature of the electron-electron correlation effect induced in a biased mesoscopic conductor.[29–31] The noise measurement clearly tells that S_1 is also not symmetric with respect to the magnetic field reversal.

Figures 4(c) and 4(d) show G_2^S and G_2^A in the left axis as a function of V_g, respectively, where S_1^S and S_1^A are superposed in the right axis. Clearly there appears strong correlation between G_2^S and S_1^S and between G_2^A and S_1^A with CF = 0.84 and 0.85, respectively. As the theory predicts that $S_1^S = 2k_BTG_2^S$ and $S_1^A = 6k_BTG_2^A$, Figs. 4(e) and 4(f) show the plots to compare between the theory and the experiment. The dotted lines are the prediction. As is consistent with the previous report,[25] the symmetric part deviates from the theory while the antisymmetric part in Fig. 4(f) is in better agreement with the theory than the symmetric one in Fig. 4(e). For the presented data set, $S_1^S/2k_BTG_2^S = 6.00^{+0.94}_{-0.98}$ and $S_1^A/6k_BTG_2^A = 1.61^{+0.22}_{-0.20}$, being statistically consistent with the previous report.[25,37] The reason for the observed considerable deviation from the theory in the symmetric part is not yet clear. We note that in a double-quantum dot experiment performed in the incoherent regime[24] similar large discrepancy

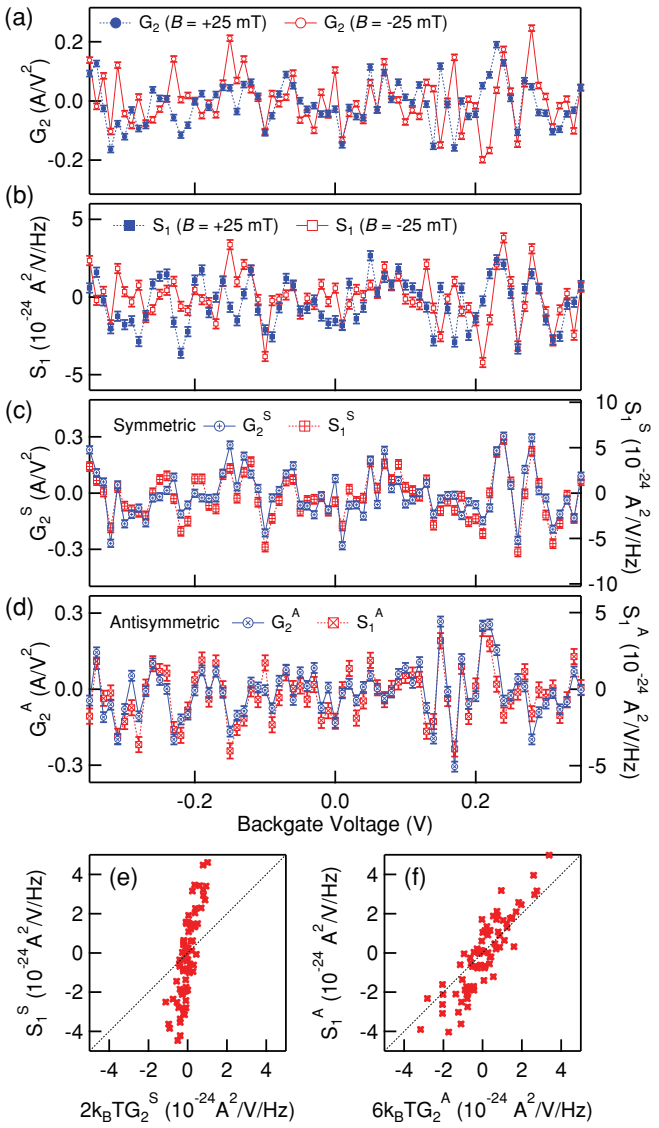

FIG. 4. (Color online) (a) G_2 obtained at $B = 25$ and -25 mT is shown as a function of V_g. (b) S_1 obtained at $B = 25$ and -25 mT is shown as a function of V_g. (c) The symmetrized components G_2^S and S_1^S are shown in the left and right axes. (d) The symmetrized components G_2^S and S_1^S are shown in the left and right axes. (e) S_1^S is plotted against $2k_BTG_2^S$. The dotted line is the prediction. (f) S_1^A is plotted against $6k_BTG_2^A$. The dotted line is the prediction.

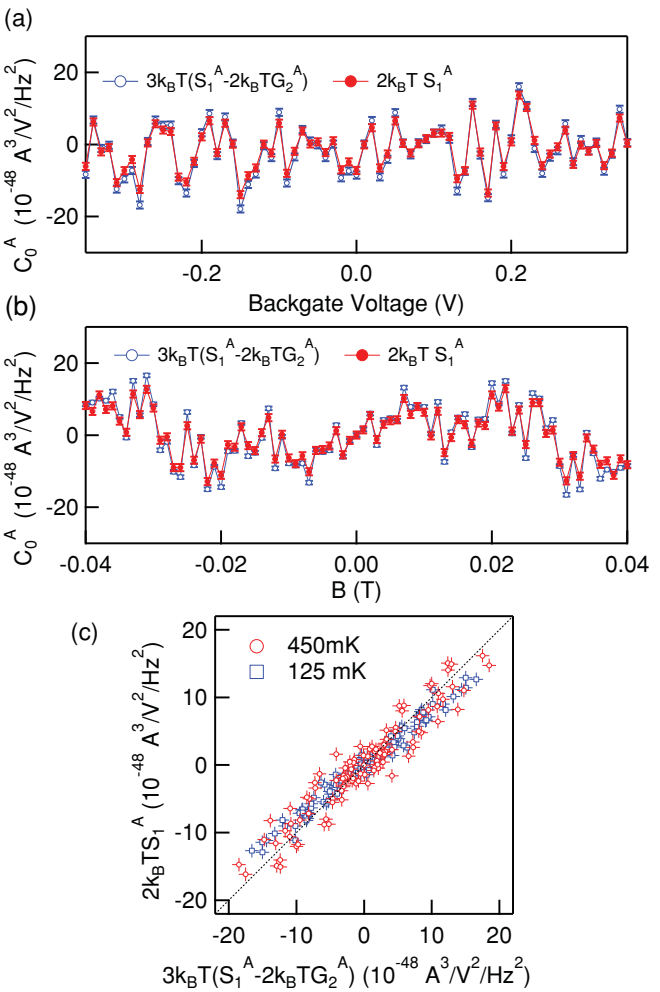

FIG. 5. (Color online) (a) Based on the data shown in Fig. 4(d) $3k_BT(S_1^A - 2k_BTG_2^A)$ and $2k_BTS_1^A$ are plotted as a function of V_g. (b) Similar plot is shown for the data set in Fig. 3 in Ref. 25. (c) $3k_BT(S_1^A - 2k_BTG_2^A)$ vs $2k_BTS_1^A$ obtained at 125 and 450 mK.

between the prediction based on FT was reported, where the back action of the nonequilibrium quantum point contact attached to the dots to detect their charge states explains the observation.[16] In the present case, as no such detector is present, further effort is necessary to solve this problem.

Regarding the amplitude of G_2^S and G_2^A, the experiment on the nonlinear transport in the AB ring fabricated on the conventional 2DEG was reported before.[30] The radius of their ring is about three times larger than ours. They measured the temperature dependence of the amplitudes G_2^S and G_2^A and found that the amplitudes rapidly decrease as temperature increases from 30 mK to 1 K. Similar temperature dependence was observed in the present ring. At the lowest temperature, the amplitude of G_2^S and G_2^A in the present case is slightly larger but falls in the same range of their result.

Now let us discuss the microreversibility in the present system. In the presence of the magnetic field, the possibility of the absence of the microreversibility in the nonequilibrium was recently pointed out.[14] While the antisymmetric relation is only given by Eq. (23), the restriction of the microreversibility simultaneously requires the relation of Eq. (22). Thus we can basically obtain C_0^A from the experimental data in two ways; by calculating $C_0^A = 3k_BT(S_1^A - 2k_BTG_2^A)$ which holds true regardless of the microreversibility condition and by calculating $C_0^A = 2k_BTS_1^A$ validated only with the microreversibility. Figure 5(a) shows the obtained C_0^A from the data set shown in Fig. 4. Clearly as a function of V_g, C_0^A calculated in two ways coincide each other. Figure 5(b) shows the result for the data reported in Fig. 3 in Ref. 25 where the field is swept with a fixed V_g. In this case too, C_0^A obtained in two ways almost perfectly equal each other.

In Fig. 5(c) we plot $3k_BT(S_1^A - 2k_BTG_2^A)$ vs $2k_BTS_1^A$ at 125 and 450 mK. As we have seen that $S_1^A/6k_BTG_2^A$ deviates from unity, the slope is slightly different from unity. However,

within the accuracy of the present experiment, we may claim that two values are the same. This tells us that in the present experiment the assumption of the microreversibility is valid.

Finally, we note that the present demonstration gives a single example of the validity of the microreversibility in the nonequilibrium quantum regime in the presence of the magnetic field. This fundamental topic should be experimentally addressed in many systems such as electron interferometers,[14,15,38] the quantum dot,[39] and the macroscopic inhomogeneous system.[40]

IV. CONCLUSIONS

We show that the fluctuation theorem is semiquantitatively valid in the description of the quantum transport in mesoscopic systems. Unlike the conventional scattering theory, this description gives a nontrivial relation between the nonlinearity and the nonequilibrium in the presence of the magnetic field. The direct test of the validity of the microreversibility was also addressed. Since the fluctuation theorem does not directly give the physical interpretation of the current through the device as the Landauer-Büttiker formalism does, both descriptions are complementary to each other. We believe that by combining these two pictures, nonequilibrium properties in mesoscopic systems in the presence of the interaction effect will be further addressed.

ACKNOWLEDGMENTS

We appreciate fruitful discussions from Markus Büttiker, Masahito Ueda, Takeo Kato, and Hisao Hayakawa. This work is partially supported by KAKENHI, Yamada Science Foundation, SCAT, Matsuo Science Foundation, Strategic International Cooperative Program the Japan Science and Technology Agency (JST), and the German Science Foundation (DFG).

*kensuke@scl.kyoto-u.ac.jp

[1] See, e.g., S. Datta, *Electronic Transport in Mesoscopic Systems* (Cambridge University Press, Cambridge, 1995); Y. Imry, *Introduction to Mesoscopic Physics* (Oxford University Press, New York, 1997).
[2] M. Büttiker, Phys. Rev. B **46**, 12485 (1992).
[3] Th. Martin and R. Landauer, Phys. Rev. B**45**, 1742 (1992).
[4] Y. M. Blanter and M. Büttiker, Phys. Rep. **336**, 1 (2000).
[5] R. de Picciotto, M. Reznikov, M. Heiblum, V. Umansky, G. Bunin, and D. Mahalu, Nature (London) **389**, 162 (1997).
[6] L. Saminadayar, D. C. Glattli, Y. Jin, and B. Etienne, Phys. Rev. Lett. **79**, 2526 (1997).
[7] X. Jehl, M. Sanquer, R. Calemczuk, and D. Mailly, Nature (London) **405**, 50 (2000).
[8] M. Esposito, U. Harbola, and S. Mukamel, Rev. Mod. Phys. **81**, 1665 (2009).
[9] D. J. Evans, E. G. D. Cohen, and G. P. Morriss, Phys. Rev. Lett. **71**, 2401 (1993).
[10] D. Andrieux, and P. Gaspard, J. Chem. Phys. **121**, 6167 (2004); J. Stat. Mech. (2006) P01011; J. Stat. Phys. **127**, 107 (2007).
[11] J. Tobiska and Yu. V. Nazarov, Phys. Rev. B **72**, 235328 (2005).
[12] D. Andrieux, P. Gaspard, T. Monnai, and S. Tasaki, New J. Phys. **11**, 043014 (2009).
[13] K. Saito and Y. Utsumi, Phys. Rev. B **78**, 115429 (2008); Y. Utsumi and K. Saito, *ibid.* **79**, 235311 (2009).
[14] H. Förster and M. Büttiker, Phys. Rev. Lett. **101**, 136805 (2008).
[15] H. Förster, and M. Büttiker, *AIP Conference Proceedings 1129, 20th International Conference on Noise and Fluctuations*, eds. M. Macucci and G. Basso, (Melville, New York, 2009), p. 443.
[16] Y. Utsumi, D. S. Golubev, M. Marthaler, K. Saito, T. Fujisawa, and G. Schön, Phys. Rev. B **81**, 125331 (2010).
[17] M. Campisi, P. Talkner, and P. Hänggi, Phys. Rev. Lett. **105**, 140601 (2010).
[18] A. Altland, A. De Martino, R. Egger, and B. Narozhny, Phys. Rev. B **82**, 115323 (2010).
[19] G. Gallavotti, Phys. Rev. Lett. **77**, 4334 (1996).
[20] G. M. Wang, E. M. Sevick, E. Mittag, D. J. Searles, and D. J. Evans, Phys. Rev. Lett. **89**, 050601 (2002).
[21] N. Garnier and S. Ciliberto, Phys. Rev. E **71**, 060101(R) (2005).
[22] J. Kurchan, e-print arXiv:cond-mat/0007360 (unpublished).
[23] S. Gustavsson, R. Leturcq, B. Simovic, R. Schleser, T. Ihn, P. Studerus, K. Ensslin, D. C. Driscoll, and A. C. Gossard, Phys. Rev. Lett. **96**, 076605 (2006).
[24] T. Fujisawa, T. Hayashi, R. Tomita, and Y. Hirayama, Science **312**, 1634 (2006).
[25] S. Nakamura, Y. Yamauchi, M. Hashisaka, K. Chida, K. Kobayashi, T. Ono, R. Leturcq, K. Ensslin, K. Saito, Y. Utsumi, and A. C. Gossard, Phys. Rev. Lett. **104**, 080602 (2010).
[26] The factor 2 is artificially introduced so that the resultant expression for S_0 and G_1 is consistent with the classical expression of the Johnson-Nyquist relation.
[27] D. Sánchez and M. Büttiker, Phys. Rev. Lett. **93**, 106802 (2004); M. L. Polianski and M. Büttiker, *ibid.* **96**, 156804 (2006); D. Sánchez and M. Büttiker, Phys. Rev. B **76**, 205308 (2007).
[28] B. Spivak and A. Zyuzin, Phys. Rev. Lett. **93**, 226801 (2004).
[29] J. Wei, M. Shimogawa, Z. Wang, I. Radu, R. Dormaier, and D. H. Cobden, Phys. Rev. Lett. **95**, 256601 (2005); D. M. Zumbühl, C. M. Marcus, M. P. Hanson, and A. C. Gossard, *ibid*. **96**, 206802 (2006); C. A. Marlow, R. P. Taylor, M. Fairbanks, I. Shorubalko, and H. Linke, *ibid.* **96**, 116801 (2006); B. Brandenstein-Köth, L. Worschech, and A. Forchel, Appl. Phys. Lett. **95**, 062106 (2009).
[30] L. Angers, E. Zakka-Bajjani, R. Deblock, S. Gueron, H. Bouchiat, A. Cavanna, U. Gennser, and M. Polianski, Phys. Rev. B **75**, 115309 (2007).
[31] R. Leturcq, D. Sánchez, G. Götz, T. Ihn, K. Ensslin, D. C. Driscoll, and A. C. Gossard, Phys. Rev. Lett. **96**, 126801 (2006); R. Leturcq, R. Bianchetti, G. Götz, T. Ihn, K. Ensslin, D. C. Driscoll, A. C. Gossard, Physica E **35**, 327 (2006).

[32] Y. Yamauchi, M. Hashisaka, S. Nakamura, K. Chida, S. Kasai, T. Ono, R. Leturcq, K. Ensslin, D. C. Driscoll, A. C. Gossard, and K. Kobayashi, Phys. Rev. B **79**, 161306(R) (2009).

[33] R. Held, T. Vancura, T. Heinzel, K. Ensslin, M. Holland, and W. Wegscheider, Appl. Phys. Lett. **73**, 262 (1998).

[34] L. DiCarlo, Y. Zhang, D. T. McClure, C. M. Marcus, L. N. Pfeiffer, and K. W. West, Rev. Sci. Instrum. **77**, 073906 (2006); M. Hashisaka, Y. Yamauchi, S. Nakamura, S. Kasai, K. Kobayashi, and T. Ono, J. Phys. Conf. Series **109**, 012013 (2008).

[35] M. Hashisaka, Y. Yamauchi, S. Nakamura, S. Kasai, T. Ono, and K. Kobayashi, Phys. Rev. B **78**, 241303(R) (2008).

[36] S. Nakamura, M. Hashisaka, Y. Yamauchi, S. Kasai, T. Ono, and K. Kobayashi, Phys. Rev. B **79**, 201308(R) (2009).

[37] To estimate the error bars of the coefficients between the two values, Passing-Bablok regression was adopted since both S_1 (S_1^S or S_1^A) and G_2 (G_2^S or G_2^A) have statistical uncertainties, where the conventional linear regression is not justified to estimate the error bars. Here the error bar indicates the 95% confidence interval. H. Passing and W. A. Bablok, J. Clin. Chem. Clin. Biochem. **21**, 709 (1983).

[38] J. S. Lim, D. Sánchez, and R. López, Phys. Rev. B **81**, 155323 (2010).

[39] D. Sánchez, Phys. Rev. B **79**, 045305 (2009).

[40] K. E. Nagaev, O. S. Ayvazyan, N. Yu. Sergeeva, and M. Büttiker, Phys. Rev. Lett. **105**, 146802 (2010).